



Comparison of a New Scheimpflug Camera and Swept-Source Optical Coherence Tomographer for Measurements of Anterior Segment Parameters

Xiaomin Huang · Xuanqiao Lin · Yizhou Yang · Jinjin Yu ·
Jiacheng Wang · Kexin Li · Yiran Wang · Giacomo Savini ·
Domenico Schiano-Lomoriello · Xingtao Zhou · Jinhai Huang

Received: July 30, 2023 / Accepted: August 31, 2023 / Published online: September 25, 2023
© The Author(s) 2023

ABSTRACT

Introduction: This study evaluated the differences and agreement between a new Scheimpflug camera (Scansys) and a swept-source anterior segment optical coherence tomographer (CASIA 2) for measurements of the anterior segment of the eye in normal subjects.

Methods: This prospective study included 84 eyes from 84 normal adult subjects who underwent three consecutive measurements with the Scansys and the CASIA 2 in random order. The mean keratometry (Km), astigmatism

magnitude (AST), J_0 , and J_{45} vectors for both anterior and posterior corneal surfaces, central corneal thickness (CCT), thinnest corneal thickness (TCT), and anterior chamber depth (ACD) were obtained by both devices. The difference between these two devices was assessed using paired t test and violin plots. Bland–Altman plots and 95% limits of agreement (LoAs) were used to evaluate agreement.

Results: No statistically significant differences between the two devices were found for the anterior AST, anterior J_{45} , and posterior J_{45} ($P > 0.05$). The remaining parameters were statistically significant ($P \leq 0.05$), but the differences not clinically significant. The violin plots showed that the distribution and probability density of the measured parameters were similar

Xiaomin Huang, Xuanqiao Lin and Yizhou Yang contributed equally as first authors.

X. Huang · J. Yu · J. Wang · K. Li · Y. Wang ·
X. Zhou · J. Huang (✉)
Eye Institute and Department of Ophthalmology
and Vision Science, Eye & ENT Hospital, Fudan
University, No.19 Baoqing Road, Xuhui District,
Shanghai 200031, China
e-mail: jinhaihuang@fudan.edu.cn;
vip999vip@163.com

X. Huang · J. Yu · J. Wang · K. Li · Y. Wang ·
X. Zhou · J. Huang
Shanghai Research Center of Ophthalmology and
Optometry, Shanghai, China

X. Lin · Y. Yang
Eye Hospital and School of Ophthalmology and
Optometry, Wenzhou Medical University,
Wenzhou, Zhejiang, China

G. Savini · D. Schiano-Lomoriello
IRCCS Bietti Foundation, Rome, Italy

X. Huang · J. Yu · J. Wang · K. Li · Y. Wang ·
X. Zhou · J. Huang
Key Laboratory of Myopia, NHC Key Laboratory of
Myopia (Fudan University), Chinese Academy of
Medical Sciences, Shanghai, China

for both devices. Bland–Altman plots revealed high agreement for the measured parameters between the Scansys and CASIA 2, with narrow 95% LoAs.

Conclusions: In terms of assessing parameters for the anterior segment, our study indicated that Scansys and CASIA 2 generally showed significant agreement. The two devices used in this study's assessment of all the parameters can be used interchangeably in refractive analysis.

Keywords: Scheimpflug camera; Swept-source optical coherence tomography; Anterior segment parameters; Agreement

Key Summary Points

Why carry out this study?

With the rising prevalence of myopia, the need for refractive surgery is increasing. Accurate measurement of the ocular anterior segment parameter is necessary for personalized surgical design and preoperative risk assessment for refractive surgery.

The study asks whether significant agreement exists between the new Scheimpflug camera (Scansys) and the swept-source anterior segment optical coherence tomographer (CASIA 2).

What was learned from the study?

In measurements of the anterior segment of the eye, our data indicates high agreement between Scansys and CASIA 2. Therefore, we suggest that all measured parameters can be considered interchangeable in refractive analysis.

INTRODUCTION

The parameters of the anterior corneal surface significantly affect corneal curvature and refractive power, which are essential during the preoperative examination for cataract and

refractive surgery [1]. In addition, the parameters of the posterior corneal surface contribute to the early diagnosis of keratoconus, corneal ectasia, and other corneal diseases [2]. Therefore, precise measurements of the anterior segment of the eye are necessary for personalized surgery design and the assessment of preoperative risk in cataract and refractive surgery [3, 4].

With the evolution of new technologies, various principles-based ocular biometers have been produced. Optical biometric devices have the advantages of being rapid and non-contact, and they are therefore widely used in the preoperative examination of corneal refractive surgery [5–7]. Devices based on reflection techniques, such as keratometers and Placido discs, can only detect the anterior surface of the cornea, but devices based on tomographic imaging techniques, such as Scheimpflug and optical coherence tomography (OCT), can detect both the anterior and posterior surfaces [8, 9]. Scheimpflug imaging has been one of the most widely used technologies, e.g. it has been applied in the Pentacam (Oculus, Wetzlar, Germany), Galilei (Ziemer Ophthalmology GmbH, Switzerland), and Sirius (CSO, Italy) devices, and its repeatability, reproducibility, and agreement with other devices are excellent [10–13]. The Scansys (MediWorks, Shanghai, China) is a new three-dimensional anterior segment biometry analyzer using the Scheimpflug imaging principle. It can provide 360° anterior segment data quickly and improve the efficiency of preoperative examination for cataract and refractive surgery.

The anterior segment OCT (AS-OCT) is a more recent imaging technology, and its high resolution and high-quality images compensate well for the shortcoming of Scheimpflug imaging [14]. The swept-source OCT (SS-OCT) technique utilizes a high-speed wavelength tuning laser, improving tissue penetration depth and signal-to-noise ratio [15]. The CASIA 2 (Tomey, Nagoya, Japan) is an improved version of the CASIA SS-1000 (Tomey, Nagoya, Japan), and represents a second-generation AS-OCT device. It has higher scanning depth, scanning density, and imaging resolution than the CASIA SS-1000 [16, 17]. A large number of studies have suggested that CASIA 2 has excellent repeatability and reproducibility in ocular biometry [18–21].

However, since the Scansys device is relatively new, there are few reports regarding its precision on ocular anterior segment parameter measurement. Therefore, this study compared the differences and agreement between Scansys and CASIA 2 in the measurement of corneal parameters in normal subjects to evaluate the clinical application value of both instruments.

METHODS

Subjects

This prospective study enrolled 84 healthy volunteers (84 right eyes) at the Eye & ENT Hospital of Fudan University. The study was conducted in accordance with the principles of the Declaration of Helsinki and was approved by the ethics committee of the Eye & ENT Hospital of Fudan University (2021174). All participants signed informed consent forms after being informed about the study's goal. The inclusion criteria were (1) subjects over 18 years of age, willing and able to participate in the measurement, (2) no history of wearing contact lenses in the short term (for soft lenses less than 2 weeks and rigid lenses less than 4 weeks), (3) corrected distance visual acuity (CDVA) $\geq 20/20$, and (4) intraocular pressure (IOP) within the normal range (10–21 mmHg). The exclusion criteria were (1) active ocular inflammation and history of ocular trauma and surgery, (2) ocular diseases such as pterygium, corneal disease, glaucoma, and vitreoretinal disease, (3) connective tissue disorders like rheumatoid arthritis and systemic lupus erythematosus, and (4) dry eyes.

Instruments

The Scansys is based on 360° rotating Scheimpflug image photography, which uses a 470 nm blue light-emitting diode (LED) slit light. The Scansys is based on 360° rotating Scheimpflug image photography, which uses a 470 nm blue LED slit light. Scansys offers two versions of their software: standard and professional. The professional version, which

generates 60 tomographic images in a single second, collects 230,400 data points, and is mainly used to optimize intraocular lenses. Our study used the standard version primarily for refractive analysis. It captures 28 anterior and posterior surface tomography pictures of the cornea in one shot, gathering 107,520 data points. The measurement ranges for the horizontal and vertical axes are up to 14 mm and 10 mm, respectively. Additionally, it can monitor the tiniest eye movements and adjust for them using a software algorithm to reduce motion inaccuracies. It provides anterior and posterior corneal topography, including elevation maps, corneal thickness maps, and corneal curvature maps [22].

The CASIA 2, an SS-OCT based biometer with a 1310 nm swept-source laser wavelength, has a scanning speed of 50,000 A-scan/s, a scanning depth of 13 mm, and a longitudinal resolution of 10 μm , and a transverse resolution of 30 μm . The anterior and posterior corneal curvatures are assessed via 16 radial scans over 0.3 s [16].

Procedures

A well-trained operator measured each participant's eyes with both instruments in random order. Each subject's eyes were measured three times in each eye. Because of the similarity of the two eyes of the same patient, only the participant's right eye was included in this study. To reduce the effect of physiological rhythm on the eye, all subjects were examined at least 3 h after waking up and opening their eyes from 10:00 AM to 4:00 PM [23, 24]. Participant were instructed to blink before each measurement to obtain an even tear film. Only measurements with an imaging quality of "OK" were accepted. The measured parameters included steep keratometry (Ks), flat keratometry (Kf), mean keratometry (Km), astigmatism magnitude (AST), central corneal thickness (CCT), thinnest corneal thickness (TCT), and anterior chamber depth (ACD).

The combination of astigmatism magnitude and axis was converted to J_0 and J_{45} vectors using the following equation [25]:

$$J_0 = -(K_s - K_f)/2 \times \cos 2\alpha$$

$$J_{45} = -(K_s - K_f)/2 \times \sin 2\alpha$$

where α represent the cylindrical axis.

Statistical Analysis

The data were analyzed using SPSS (21.0, IBM Corp, USA) and Excel (v365, Microsoft Corp, USA). Because the Kolmogorov–Smirnov test revealed that all of the data had a normal distribution, the results were reported as mean \pm standard deviation (SD). As a hybrid of box plots and kernel density plots, violin plots (GraphPad Prism 8, CA, USA) depict the distributions and density of the measured parameters. To determine whether the mean difference between the parameters measured by the two devices was statistically significant, the paired *t* test was performed; $P \leq 0.05$ was considered statistically significant. Bland–Altman plots and the 95% limits of agreement (95% LoAs) were used to assess the agreement between the two devices. The 95% LoAs was defined as the average difference between the two devices ± 1.96 SD.

RESULTS

A total of 84 right eyes of healthy subjects were analyzed in this prospective study. The male to female ratio was 1:2.2. The mean age was 28 ± 6.4 years (range 18–47 years).

All CDVA values were better than 20/20 Snellen equivalent. The spherical refraction was -4.57 ± 2.35 diopters (D) (range -9.25 to -0.50 D) and cylinder was -0.63 ± 0.71 D (range -1.25 to -2.75 D).

Table 1 and show the difference and agreement of the measured parameters between Scansys and CASIA 2. There were no statistically significant ($P > 0.05$) differences in the anterior AST, anterior J_{45} , and posterior J_{45} values measured between Scansys and CASIA 2. Despite being statistically significant ($P < 0.05$), the differences in the remaining parameters between the two devices were minor. Scansys values for CCT, TCT, posterior AST, and

posterior J_0 were slightly larger than those obtained by CASIA 2, while the remaining parameters were lower than those measured by CASIA 2. Figure 1 shows the distinct expression patterns of the two devices, indicating that the distribution and probability density of the measured parameters are similar for both devices. The Bland–Altman plots revealed narrow 95% LoAs for the parameters measured by Scansys and CASIA 2 devices (Figs. 2, 3, 4, 5).

DISCUSSION

The Scansys, a new anterior segment analyzer, is based on the Scheimpflug imaging principle and can simultaneously acquire anterior and posterior corneal surface, iris, and lens data. Scansys has received little prior research, with only a few studies comparing it to Pentacam [22, 26]; no agreement studies with other instruments are available. As far as we know, this is the first study to compare the agreement of Scansys with an SS-OCT-based biometer. In addition to conventional statistical methods, violin plots were used to visually describe the distribution and density of the measured parameters in our study. The results confirmed that the parameters obtained by Scansys are in excellent agreement with those measured by CASIA 2 and can be used interchangeably in refractive analysis.

In the current study, the CCT and TCT measured by Scansys were slightly larger than those measured by CASIA 2, with a mean difference of $13.45 \mu\text{m}$ and $15.68 \mu\text{m}$, respectively ($P < 0.001$). Our results are consistent with those of Li et al., in which CCT measured using Pentacam was higher than that of CASIA 2 with a mean difference of $9.64 \mu\text{m}$ [27]. Kiraly et al. showed that the Pentacam exhibited a thicker CCT than the IOLMaster 700, with a mean difference of $10.99 \mu\text{m}$ [28]. Corneal thickness measurements with the Scheimpflug technique were generally higher than with SS-OCT, which may be because SS-OCT technology better distinguishes the anterior–posterior border of the cornea [24], and Scheimpflug may include the tear film in the corneal thickness measurement [29]. In the current study, the maximum

Table 1 Means values and distribution for parameters measured by Scansys vs. CASIA 2

Parameters	Scansys			CASIA 2		
	Mean ± SD	Minimum	Maximum	Mean ± SD	Minimum	Maximum
CCT (µm)	546.68 ± 31.95	477.00	626.33	533.23 ± 32.32	462.67	616.33
TCT (µm)	543.28 ± 32.16	473.67	622.67	527.60 ± 32.56	459.00	610.33
ACD (mm)	3.19 ± 0.26	2.56	3.70	3.24 ± 0.26	2.69	3.80
Anterior Km (D)	42.99 ± 1.28	39.48	45.90	43.24 ± 1.28	39.75	46.17
Anterior AST (D)	1.09 ± 0.69	0.13	3.20	1.10 ± 0.65	0.13	3.03
Anterior J_0 (D)	- 0.45 ± 0.37	- 1.59	0.12	- 0.49 ± 0.35	- 1.52	0.28
Anterior J_{45} (D)	0.06 ± 0.26	- 0.52	0.88	0.08 ± 0.21	- 0.51	0.73
Posterior Km (D)	- 6.06 ± 0.18	- 6.45	- 5.56	- 6.11 ± 0.17	- 6.48	- 5.65
Posterior AST (D)	- 0.34 ± 0.12	- 0.63	- 0.13	- 0.32 ± 0.13	- 0.60	- 0.03
Posterior J_0 (D)	0.16 ± 0.06	0.03	0.31	0.15 ± 0.06	0.01	0.30
Posterior J_{45} (D)	- 0.03 ± 0.04	- 0.14	0.08	- 0.03 ± 0.04	- 0.11	0.07

CCT central corneal thickness, TCT thinnest corneal thickness, ACD anterior chamber depth, Km mean keratometry, AST astigmatism, SD standard deviation, J_0 corneal astigmatism vector along the 0° meridian, J_{45} corneal astigmatism vector along the 45° meridian

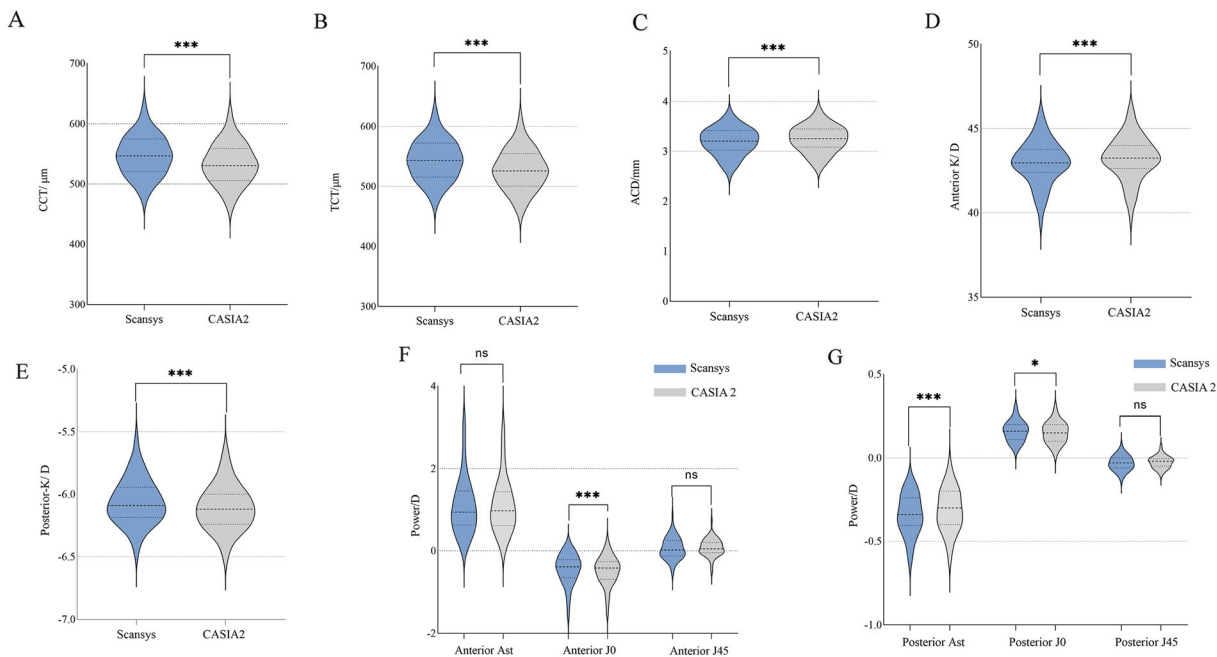


Fig. 1 Violin plots comparing measurements by Scansys and CASIA 2 in central corneal thickness (CCT) (a), thinnest corneal thickness (TCT) (b), anterior chamber depth (ACD) (c), anterior keratometry (Km) (d), posterior Km (e), anterior astigmatism (AST), anterior J_0 , anterior J_{45} (f), posterior AST, posterior J_0 , and posterior J_{45} (g). The top

and bottom black dashed lines reflect interquartile spacing whereas the black dashed line in the middle represents the median. Asterisks indicate significant differences at * $P \leq 0.05$, ** $P \leq 0.01$, *** $P \leq 0.001$; ns, nonsignificant $P > 0.05$. J_0 corneal astigmatism vector along the 0° meridian, J_{45} corneal astigmatism vector along the 45° meridian

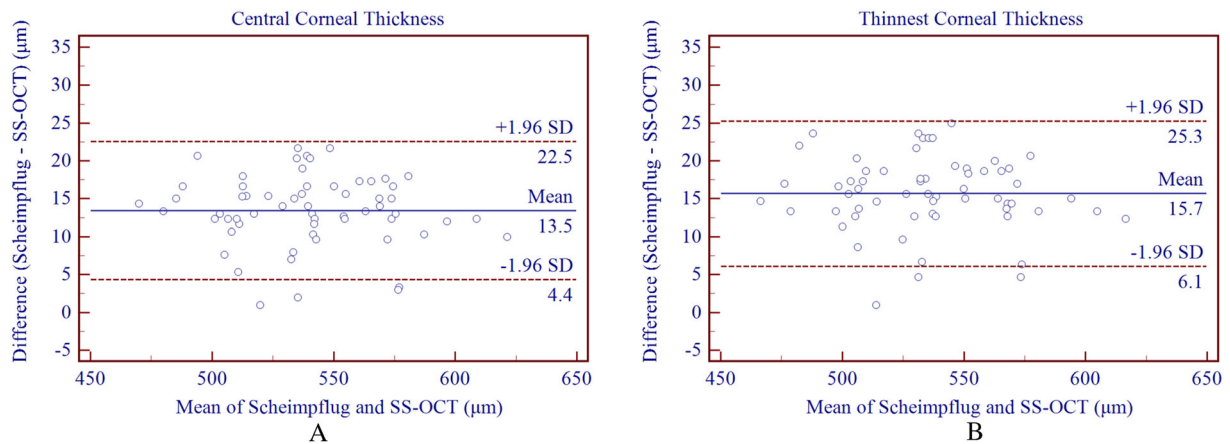


Fig. 2 Bland–Altman plots demonstrating agreement in the assessment of central corneal thickness (CCT) (a) and thinnest corneal thickness (TCT) (b) between Scansys and

CASIA 2. SS-OCT swept-source optical coherence tomography, SD standard deviation

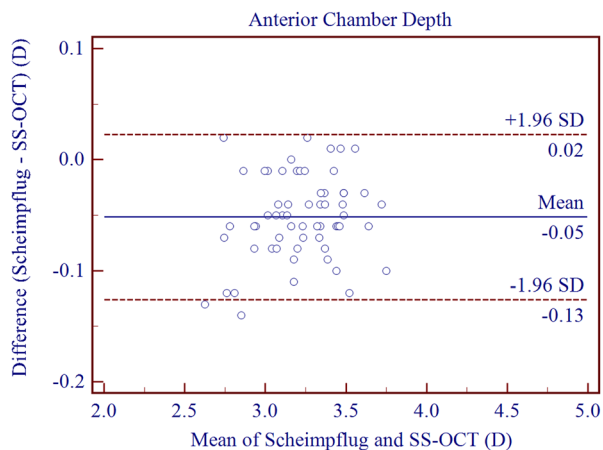


Fig. 3 Bland–Altman plots demonstrating agreement in the assessment of anterior chamber depth (ACD) between Scansys and CASIA 2. SS-OCT swept-source optical coherence tomography, SD standard deviation

absolute value of 95% LoAs of CCT and TCT were 22.55 μm and 25.28 μm , respectively. Previous studies have shown that a 10% difference in CCT measurements may result in a 3.4 ± 0.9 mmHg change in IOP measurements [30]. Therefore, considering the mean CCT of normal eyes is 536 ± 31 μm [31], the measurement differences between the Scansys and CASIA 2 correspond to a 5.02% CCT measurement difference; this result has a negligible effect on IOP. Biswas and Biswas found good agreement between the CASIA SS-1000 and

Pentacam on CCT and TCT, with 95% LoAs ranging from 1.98 to -25.42 μm and 1.72 to -24.99 μm , respectively [24]. Chen et al. compared the Pentacam and a Fourier domain optical coherence tomographer (RTVue-100; Optovue Inc, Fremont, CA, USA) for CCT and found 95% LoAs ranging between -0.7 and 22.5 μm [32]. Our results are comparable to theirs, indicating good agreement in the measurements of CCT and TCT.

For intraocular lens (IOL) power calculation, every 0.10 mm change in ACD results in a 0.10 to 0.15 D change in refraction [33]. In our study, the mean ACD value measured by Scansys was smaller than those measured by CASIA 2, with a mean difference of -0.05 mm. This difference is small and would not significantly affect the IOL power calculation. Our results are similar to those reported by Sel et al., in which the mean difference in ACD measurements between Pentacam AXL (Oculus Optikgeräte GmbH, Germany) and IOLMaster 700 was 0.04 ± 0.02 mm [34]. In the current study, the 95% LoAs for ACD were narrower, ranging from -0.13 to 0.02 mm. Özyo and Özyo found high agreement between ACD measured by the IOLMaster 700 and Pentacam with a 95% LoAs of -0.08 – 0.09 mm [35]. Li et al. used Pentacam and CASIA 2 to measure ACD with a 95% LoAs of -0.38 to 0.23 mm, also indicating excellent agreement between

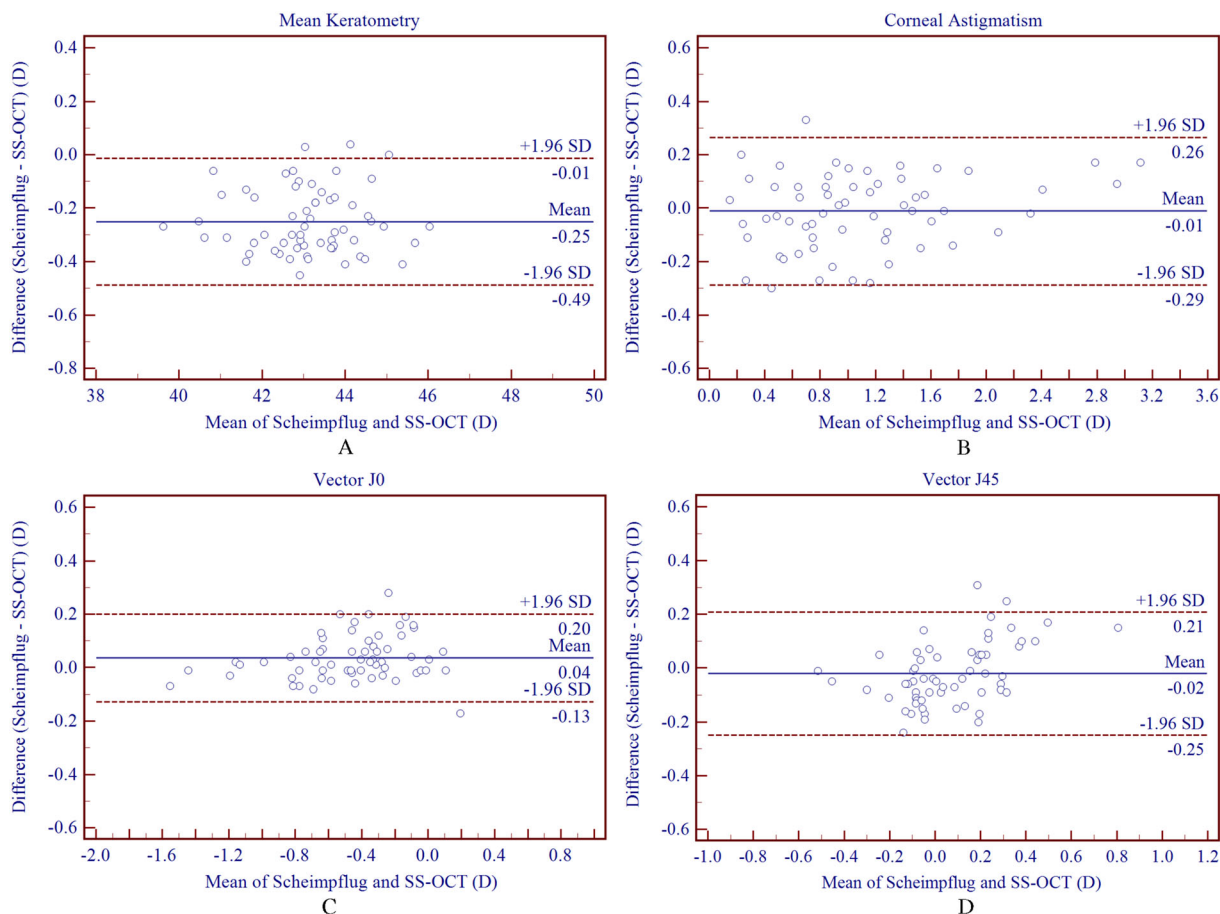


Fig. 4 Bland–Altman plots demonstrating agreement in the assessment of mean keratometry (Km) (a), astigmatism (AST) (b), J_0 (c), and J_{45} (d) of anterior corneal surface between Scansys and CASIA 2. SS-OCT swept-source optical coherence

tomography, SD standard deviation, J_0 corneal astigmatism vector along the 0° meridian, J_{45} corneal astigmatism vector along the 45° meridian

the two devices [27]. The 95% LoAs in this study were comparable to or even narrower than the above results, so Scansys has the same high level of agreement as CASIA 2.

Measurement and analysis of corneal curvature are widely used in corneal refractive surgery, IOL power calculation, corneal transplantation, and the diagnosis of keratoconus. In the current study, the difference in Km values on the anterior and posterior corneal surfaces measured by the two devices was -0.25 D and 0.05 D, respectively, which was small and clinically acceptable. Our findings were consistent with Pérez-Bartolomé et al., who found that the difference between the anterior and posterior Km measured using

Pentacam and Anterior (Heidelberg Engineering) was -0.13 D and -0.16 D, respectively [36]. The different methods and algorithms of corneal curvature measurement can explain the difference between the two devices. Scansys uses the Scheimpflug method to measure the height of the cornea and triangulation to turn the height data into data about the shape of the cornea [37]. In contrast, CASIA 2 is based on SS-OCT, and measurements are made by scanning two-dimensional cross-sectional maps to compose a simulated corneal surface. According to the Bland–Altman plots, the maximum absolute values of 95% LoAs on the anterior and posterior Km in this study were 0.49 D and 0.12 D. According to Eibschitz-Tsimhoni’s study

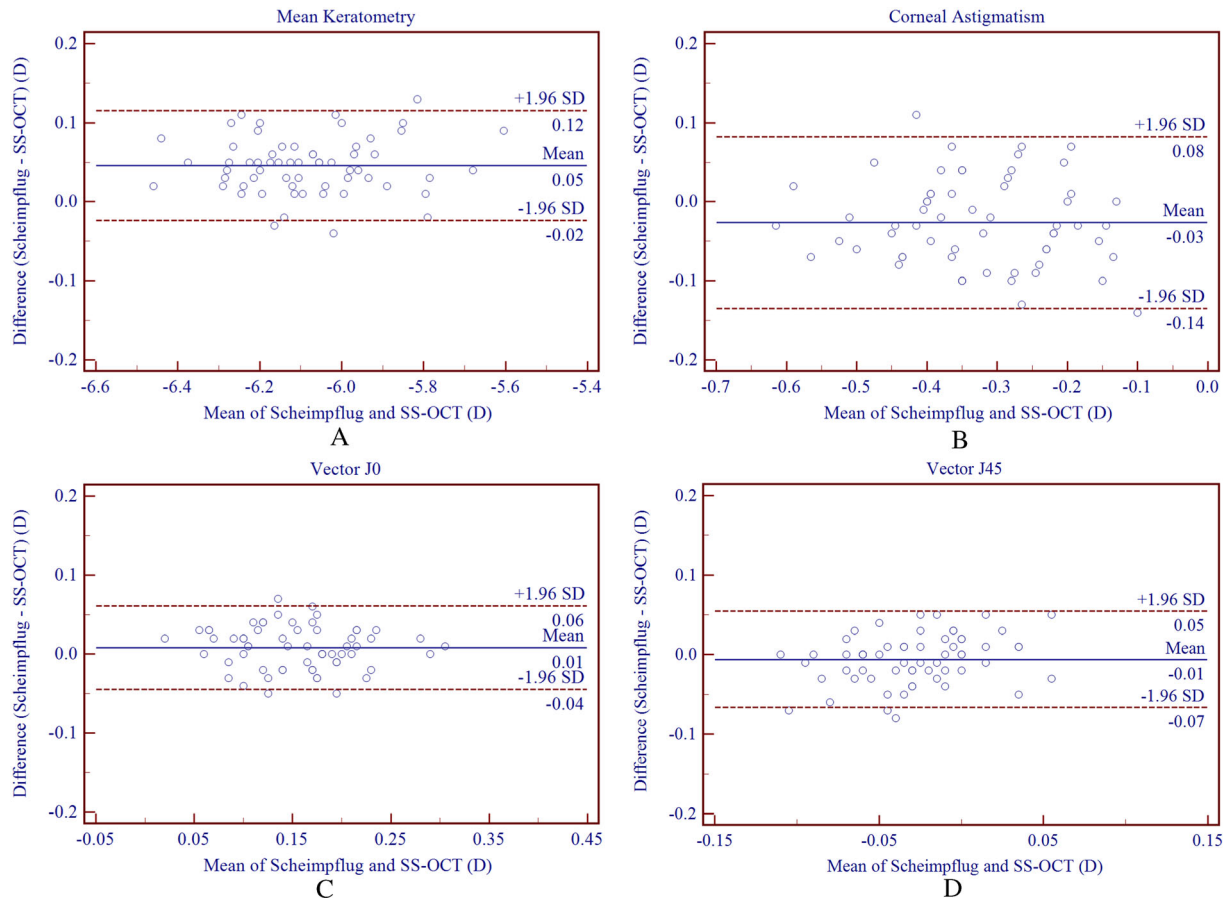


Fig. 5 Bland–Altman plots demonstrating agreement in the assessment of mean keratometry (Km) (a), astigmatism (AST) (b), J_0 (c), and J_{45} (d) of posterior corneal surface between Scansys and CASIA 2. SS-OCT swept-source

optical coherence tomography, SD standard deviation, J_0 corneal astigmatism vector along the 0° meridian, J_{45} corneal astigmatism vector along the 45° meridian

[38], every 1.00 D deviation in corneal curvature results in a 0.80 to 1.30 D deviation in IOL power calculation, and an error margin of 0.5 D is acceptable in clinical applications; therefore, the 95% LoAs of Km in this study is clinically acceptable, though constant optimization would still be highly recommended. Many previous studies have demonstrated that measurements from different corneal curvature measurement systems cannot be considered interchangeable. Cui et al., for example, compared color LED technology (Cassini, Casini Technologies, the Hague, the Netherlands) to Pentacam with a 95% LoAs ranging from -0.60 to 0.76 D for anterior Km [39]. The study by Crawford et al. also suggests that Orbscan II and Pentacam tomographers differ significantly and

are not yet interchangeable for clinical use [40]. In contrast, the OCT system and Scheimpflug camera, which simultaneously measure the anterior and posterior corneal curvature, had high agreement in most studies and were consistent with our findings. Zhao et al. reported excellent agreement between the Km values measured by Pentacam and CASIA SS-1000 in children, with a 95% LoAs ranging from -0.09 to 0.51 D [41]. High agreement was found between CASIA and Pentacam HR (95% LoAs, -0.24 to 0.54 D) in adults [42]. As a result, the anterior and posterior Km measured by the two devices also showed high agreement.

Accurate measurement of preoperative AST is an integral part of good postoperative monitoring of visual quality in patients. We found

Table 2 Difference and agreement for parameters measured by Scansys vs. CASIA 2

Parameters	Mean difference \pm SD	<i>P</i> value	95% LoAs
CCT (μm)	13.45 \pm 4.64	< 0.001	4.36 to 22.55
TCT (μm)	15.68 \pm 4.90	< 0.001	6.08 to 25.28
ACD (mm)	− 0.05 \pm 0.04	< 0.001	− 0.13 to 0.02
Anterior Km (D)	− 0.25 \pm 0.12	< 0.001	− 0.49 to − 0.01
Anterior AST (D)	− 0.01 \pm 0.14	0.532	− 0.29 to 0.26
Anterior J_0 (D)	0.04 \pm 0.08	0.001	− 0.13 to 0.20
Anterior J_{45} (D)	− 0.02 \pm 0.12	0.177	− 0.25 to 0.21
Posterior Km (D)	0.05 \pm 0.04	< 0.001	− 0.02 to 0.12
Posterior AST (D)	− 0.03 \pm 0.06	< 0.001	− 0.14 to 0.08
Posterior J_0 (D)	0.01 \pm 0.03	0.021	− 0.04 to 0.06
Posterior J_{45} (D)	− 0.01 \pm 0.03	0.139	− 0.07 to 0.05

CCT central corneal thickness, *TCT* thinnest corneal thickness, *ACD* anterior chamber depth, *Km* mean keratometry, *AST* astigmatism, *SD* standard deviation, J_0 corneal astigmatism vector along the 0° meridian, J_{45} corneal astigmatism vector along the 45° meridian

that the average difference between AST, J_0 , and J_{45} measured by the two instruments was small, ranging between − 0.03 and 0.04 D. The distribution and density of the violin plots were similar. Furthermore, the maximum absolute 95% LoAs for anterior and posterior surface AST, J_0 , and J_{45} were all less than 0.3 D, with high agreement. Similarly, Gim et al. used Pentacam and Anterior to measure anterior and posterior corneal J_0/J_{45} , obtaining a narrow 95% LoAs range, which showed high agreement [43]. The study by Zhao et al. compared J_0 and J_{45} between Pentacam and CASIA SS-1000. The maximum absolute 95% LoAs for J_0 was 0.23 D, and that for J_{45} was 0.31 D [41]. Özyo and Özyo compared Pentacam and IOLMaster 700 for J_0 (95% LoAs of 0.24 to − 0.1 D) and J_{45} (95% LoAs of 0.27 to − 0.31 D), both of which can be used interchangeably [35].

There were some limitations in this study. First, we did not include other parameters, such as iridocorneal angle, crystalline lens, and pupil parameters. We will compare more parameters in the future. Another constraint was that we only included healthy eyes. Further research should be conducted to compare different groups of patients, particularly those excluded

from the study because of corneal ectatic and corneal disease.

CONCLUSION

Our data show a high agreement between Scansys and CASIA 2 in healthy subjects for ACD, CCT, TCT, Km anterior, Km posterior, AST anterior, AST posterior, J_0 anterior, J_0 posterior, J_{45} anterior, and J_{45} posterior. Therefore, we suggest that all measured parameters can be considered interchangeable in refractive analysis.

Author Contributions. Design of the study (Xiaomin Huang, Xuanqiao Lin, Yizhou Yang, Xingtao Zhou and Jinhai Huang); conduct of the study (Xiaomin Huang, Xuanqiao Lin, Yizhou Yang, and Jinjin Yu); data collection (Jinjin Yu, Jiacheng Wang, Kexin Li and Yiran Wang); analysis and interpretation (Xiaomin Huang, Xingtao Zhou and Jinhai Huang); manuscript preparation and review (Xiaomin Huang, Xuanqiao Lin, Giacomo Savini, Domenico Schiano-Lomoriello, Xingtao Zhou and Jinhai

Huang); read and approved the final version of the article (Xiaomin Huang, Xuanqiao Lin, Yizhou Yang, Jinjin Yu, Jiacheng Wang, Kexin Li, Yiran Wang, Giacomo Savini, Domenico Schiano-Lomoriello, Xingtao Zhou and Jinhai Huang).

Funding. This work was supported in part by the Project of National Natural Science Foundation of China (Grant No. 82271048); Shanghai Science and Technology (Grant No. 22S11900200, 23XD1420500); EYE & ENT Hospital of Fudan University High-level Talents Program (Grant No. 2021318); Clinical Research Plan of SHDC (Grant No. SHDC2020CR1043B); Project of Shanghai Xuhui District Science and Technology (Grant No. 2020–015); Program for Professor of Special Appointment (Eastern Scholar, TP2022046) at Shanghai Institutions of Higher Learning; The contribution of IRCCS Bietti Foundation was supported by Fondazione Roma and the Italian Ministry of Health. The funders had no role in study design, data collection and analysis, decision to publish, or reparation of the manuscript. The Rapid Service Fee was funded by the authors.

Data Availability. The datasets generated during and/or analyzed during the current study are available from the corresponding author on reasonable request.

Declarations

Conflict of Interest. Xiaomin Huang, Xuanqiao Lin, Yizhou Yang, Jinjin Yu, Jiacheng Wang, Kexin Li, Yiran Wang, Giacomo Savini, Domenico Schiano-Lomoriello, Xingtao Zhou, and Jinhai Huang have nothing to disclose.

Ethical Approval. The authors are accountable for all aspects of the work. This includes ensuring that questions related to the accuracy or integrity of any part of the work are appropriately investigated and resolved. The trial was conducted in accordance with the Declaration of Helsinki. The study was approved by Ethics Committee of the Eye and ENT Hospital of Fudan University (2021174) and informed consent was obtained from all individual participants.

Open Access. This article is licensed under a Creative Commons Attribution-NonCommercial 4.0 International License, which permits any non-commercial use, sharing, adaptation, distribution and reproduction in any medium or format, as long as you give appropriate credit to the original author(s) and the source, provide a link to the Creative Commons licence, and indicate if changes were made. The images or other third party material in this article are included in the article's Creative Commons licence, unless indicated otherwise in a credit line to the material. If material is not included in the article's Creative Commons licence and your intended use is not permitted by statutory regulation or exceeds the permitted use, you will need to obtain permission directly from the copyright holder. To view a copy of this licence, visit <http://creativecommons.org/licenses/by-nc/4.0/>.

REFERENCES

1. Müller LJ, Pels E, Vrensen GFJM. The specific architecture of the anterior stroma accounts for maintenance of corneal curvature. *Br J Ophthalmol.* 2001;85:437–43.
2. Ambrósio R, Correia FF, Lopes B, et al. Corneal biomechanics in ectatic diseases: refractive surgery implications. *Open Ophthalmol J.* 2017;11:176–93.
3. Jin H, Ou Z, Guo H, Zhao P. Myopic laser corneal refractive surgery reduces interdevice agreement in the measurement of anterior corneal curvature. *Eye Contact Lens.* 2018;44(Suppl 1):S151–7.
4. Hamer CA, Buckhurst H, Purslow C, Shum GL, Habib NE, Buckhurst PJ. Comparison of reliability and repeatability of corneal curvature assessment with six keratometers. *Clin Exp Optom.* 2016;99: 583–9.
5. Srivannaboon S, Chirapapaisan C, Chonpimai P, Locket S. Clinical comparison of a new swept-source optical coherence tomography-based optical biometer and a time-domain optical coherence tomography-based optical biometer. *J Cataract Refract Surg.* 2015;41:2224–32.
6. Wang X, Wu Q. Investigation of the human anterior segment in normal chinese subjects using a dual Scheimpflug analyzer. *Ophthalmology.* 2013;120:703–8.

7. Tang M, Chen A, Li Y, Huang D. Corneal power measurement with Fourier-domain optical coherence tomography. *J Cataract Refract Surg.* 2010;36:2115–22.
8. Chalkiadaki E, Gartaganis PS, Ntravalias T, Giannakis I, Manousakis E, Karmiris E. Agreement in anterior segment measurements between swept-source and Scheimpflug-based optical biometries in keratoconic eyes: a pilot study. *Ther Adv Ophthalmol.* 2022;14:1–15.
9. Savini G, Barboni P, Carbonelli M, Hoffer KJ. Accuracy of corneal power measurements by a new Scheimpflug camera combined with Placido-disk corneal topography for intraocular lens power calculation in unoperated eyes. *J Cataract Refract Surg.* 2012;38:787–92.
10. Rabsilber TM, Khoramnia R, Auffarth GU. Anterior chamber measurements using Pentacam rotating Scheimpflug camera. *J Cataract Refract Surg.* 2006;32:456–9.
11. Jahadi Hosseini HR, Katbab A, Khalili MR, Abtahi MB. Comparison of corneal thickness measurements using Galilei, HR Pentacam, and ultrasound. *Cornea.* 2010;29:1091.
12. Shirayama M, Wang L, Weikert MP, Koch DD. Comparison of corneal powers obtained from 4 different devices. *Am J Ophthalmol.* 2009;148:528–535.e1.
13. De la Parra-Colín P, Garza-León M, Barrientos-Gutierrez T. Repeatability and comparability of anterior segment biometry obtained by the Sirius and the Pentacam analyzers. *Int Ophthalmol.* 2014;34:27–33.
14. Savini G, Schiano-Lomoriello D, Hoffer KJ. Repeatability of automatic measurements by a new anterior segment optical coherence tomographer combined with Placido topography and agreement with 2 Scheimpflug cameras. *J Cataract Refract Surg.* 2018;44:471–8.
15. Montés-Micó R, Pastor-Pascual F, Ruiz-Mesa R, Tañá-Rivero P. Ocular biometry with swept-source optical coherence tomography. *J Cataract Refract Surg.* 2021;47:802–14.
16. Shoji T, Kato N, Ishikawa S, et al. In vivo crystalline lens measurements with novel swept-source optical coherent tomography: an investigation on variability of measurement. *BMJ Open Ophthalmol.* 2017;1: e000058.
17. Ruan X, Yang G, Xia Z, et al. Agreement of anterior segment parameter measurements with CASIA 2 and IOLMaster 700. *Front Med.* 2022;9: 777443.
18. Xu BY, Mai DD, Penteado RC, Saunders L, Weinreb RN. Reproducibility and agreement of anterior segment parameter measurements obtained using the CASIA2 and spectralis OCT2 optical coherence tomography devices. *J Glaucoma.* 2017;26:974.
19. Zhang T, Zhou Y, Young CA, Chen A, Jin G, Zheng D. Comparison of a new swept-source anterior segment optical coherence tomography and a Scheimpflug camera for measurement of corneal curvature. *Cornea.* 2020;39:818.
20. Fukuda S, Ueno Y, Fujita A, et al. Comparison of anterior segment and lens biometric measurements in patients with cataract. *Graefes Arch Clin Exp Ophthalmol.* 2020;258:137–46.
21. Wylegała A, Mazur R, Bolek B, Wylegała E. Reproducibility, and repeatability of corneal topography measured by Revo NX, Galilei G6 and Casia 2 in normal eyes. *PLoS ONE.* 2020;15: e0230589.
22. Yu A-Y, Ye J, Savini G, et al. Reliability and agreement of the central and mid-peripheral corneal thickness measured by a new Scheimpflug based imaging. *Ann Transl Med.* 2021;9:1136.
23. Lattimore MR, Kaupp S, Schallhorn S, Lewis R. Orbscan pachymetry: implications of a repeated measures and diurnal variation analysis. *Ophthalmology.* 1999;106:977–81.
24. Biswas S, Biswas P. Agreement and repeatability of corneal thickness and radius among three different corneal measurement devices. *Optom Vis Sci.* 2021;98:1196.
25. Thibos LN, Wheeler W, Horner D. Power vectors: an application of fourier analysis to the description and statistical analysis of refractive error. *Optom Vis Sci.* 1997;74:367.
26. Xu W, Zhai C, Yusufu M, et al. Repeatability and agreement between a reference Scheimpflug tomographer and a low-cost Scheimpflug system. *J Cataract Refract Surg.* 2023;49:614–9.
27. Li X, Zhou Y, Young CA, Chen A, Jin G, Zheng D. Comparison of a new anterior segment optical coherence tomography and Oculus Pentacam for measurement of anterior chamber depth and corneal thickness. *Ann Transl Med.* 2020;8:857.
28. Kiraly L, Stange J, Kunert KS, Sel S. Repeatability and agreement of central corneal thickness and keratometry measurements between four different devices. *J Ophthalmol.* 2017;2017:6181405.
29. Schröder S, Mäurer S, Eppig T, Seitz B, Rubly K, Langenbacher A. Comparison of corneal tomography: repeatability, precision, misalignment, mean

- elevation, and mean pachymetry. *Curr Eye Res.* 2018;43:709–16.
30. Kaushik S, Pandav S. Clinical science structure measuring intraocular pressure: how important is the central corneal thickness? *J Curr Glaucoma Pract.* 2007;1:21–4.
 31. Doughty MJ, Zaman ML. Human corneal thickness and its impact on intraocular pressure measures: a review and meta-analysis approach. *Surv Ophthalmol.* 2000;44:367–408.
 32. Chen S, Huang J, Wen D, Chen W, Huang D, Wang Q. Measurement of central corneal thickness by high-resolution Scheimpflug imaging, Fourier-domain optical coherence tomography and ultrasound pachymetry. *Acta Ophthalmol.* 2012;90:449–55.
 33. Olsen T. Sources of error in intraocular lens power calculation. *J Cataract Refract Surg.* 1992;18:125–9.
 34. Sel S, Stange J, Kaiser D, Kiraly L. Repeatability and agreement of Scheimpflug-based and swept-source optical biometry measurements. *Cont Lens Anterior Eye.* 2017;40:318–22.
 35. Özyol P, Özyol E. Agreement between swept-source optical biometry and Scheimpflug-based topography measurements of anterior segment parameters. *Am J Ophthalmol.* 2016;169:73–8.
 36. Pérez-Bartolomé F, Rocha-De-Lossada C, Sánchez-González J-M, Feu-Basilio S, Torras-Sanvicens J, Peraza-Nieves J. Anterior-segment swept-source ocular coherence tomography and Scheimpflug imaging agreement for keratometry and pupil measurements in healthy eyes. *J Clin Med.* 2021;10:5789.
 37. Belin MW, Khachikian SS. An introduction to understanding elevation-based topography: how elevation data are displayed - a review. *Clin Exp Ophthalmol.* 2009;37:14–29.
 38. Eibschitz-Tsimhoni M, Tsimhoni O, Archer SM, Del Monte MA. Effect of axial length and keratometry measurement error on intraocular lens implant power prediction formulas in pediatric patients. *J AAPOS.* 2008;12:173–6.
 39. Cui X-H, Yoo Y-S, An Y, Joo C-K. Comparison of keratometric measurements between color light-emitting diode topography and Scheimpflug camera. *BMC Ophthalmol.* 2019;19:98.
 40. Crawford AZ, Patel DV, McGhee CNJ. Comparison and repeatability of keratometric and corneal power measurements obtained by orbscan II, pentacam, and Galilei corneal tomography systems. *Am J Ophthalmol.* 2013;156:53–60.
 41. Zhao Y, Chen D, Savini G, et al. The precision and agreement of corneal thickness and keratometry measurements with SS-OCT versus Scheimpflug imaging. *Eye Vis.* 2020;7:32.
 42. Ghoreishi SM, Mortazavi SAA, Abtahi Z-A, et al. Comparison of Scheimpflug and swept-source anterior segment optical coherence tomography in normal and keratoconus eyes. *Int Ophthalmol.* 2017;37:965–71.
 43. Gim Y, Jun RM, Han KE. Agreement between Scheimpflug camera and the swept-source optical coherence tomography measurements in keratometry and higher-order aberrations. *Korean J Ophthalmol.* 2021;35:337–48.